Journal of Materials Chemistry A

RSC Publishing

PAPER

View Article Online
View Journal | View Issue

Cite this: J. Mater. Chem. A, 2013, 1, 10836

Self-assembly of cyclodextrin–oil inclusion complexes at the oil–water interface: a route to surfactant-free emulsions†

Baghali G. Mathapa and Vesselin N. Paunov*

We investigated the self-assembly of cyclodextrin (CD) molecules at the tetradecane–aqueous solution interface through formation of inclusion complexes (ICs). We studied the surface activity of CDs at both the air–water and the oil–water interface. Although α-CD and β-CD are not surface active at the air–water interface, they form pseudo-surfactants as inclusion complexes with linear oil molecules at the oil–water interface. We discussed the factors affecting the formation of these ICs and their assembly into microcrystals at the oil–water interface. We discovered that the morphology and the size of the aggregates formed by these ICs are dependent on the type of CD and oil used. Lamella sheets and long microrods were obtained from α-CD molecules and tetradecane. In contrast, β-CD–tetradecane gave short microrods which assembled in microcrystals. We characterised the CD–tetradecane ICs using optical microscopy, SEM, TEM and FT-IR. The crystallinity of the ICs was assessed using cross-polarised light microscopy. We demonstrated the spontaneous formation of a dense layer of adsorbed CD–tetradecane IC microcrystals at the tetradecane–water interface. At large oil volume fractions, this phenomenon led to the formation of a Pickering type of oil-in-water emulsion stabilised by adsorbed CD–oil microcrystals while at low oil volume fractions it completely solubilises the oil in the form of IC microcrystals. This emulsion stabilisation mechanism with sustainable materials like CDs may find applications in surfactant free pharmaceutical and cosmetic formulations reducing the release of surfactants in the environment.

Received 29th May 2013
Accepted 10th July 2013

DOI: 10.1039/c3ta12108a

www.rsc.org/MaterialsA

Introduction

The design of functional nanomaterials is a subject of great interest because of their unique properties and potential applications in a wide range of fields such as medical formulations, agrochemicals, skin care/cosmetics and pharmaceuticals. Click chemistry and spontaneous self-assembly are one of the promising bottom-up approaches to form supramolecular nanomaterials from molecular building blocks by non-covalent interactions such as van der Waals and hydrogen bonding.[1,2] Such self-assembly processes are reversible and simpler compared to the systems involving covalent bonds.[3] Cyclodextrins (CDs) are widely used as host molecules which can form supramolecular structures. CDs are cyclic sugars derived from hydrolysis of starch by Cyclodextrin Glycosyl Transferase bacterial enzyme (CG-Tase) consisting of six (α), seven (β) and eight (γ) glucose units bridged through 1,4-glycosidic bonds.[4,5] They have a cone shaped chemical structure with a hydrophobic inner cavity which allows CDs to incorporate other molecules through non-covalent interactions forming host–guest inclusion complexes (ICs). ICs are formed through a combination of size and geometric compatibility, van der Waals forces, and hydrophobic interactions between the CD cavity and the guest molecule.[6] A whole small molecule or parts of a large molecule can be included in the CD cavity. The threading of several CDs onto a polymer chain results in a supramolecular "nano-necklace" often named pseudopolyrotaxane (PPR).[7,8] This threading of several CD units onto a polymeric chain and close packing of CDs is aided by hydrogen bonding between the hydroxyl groups situated along the rims of the neighbouring CDs. The included polymer segments are segregated from the neighbouring polymer chains by the walls of the CD cavities and are forced to adopt highly extended conformations by the narrow host CD channels.[9] The molecular "nano-necklace" may also be grown into 3D structures through formation of hydrogen bonds from hydroxyl groups on CD units between neighbouring molecular necklaces. The end capping of PPR with bulky molecules prevents CD units from slipping off thus giving rise to polyrotaxane.[10]

CDs have different hydrophobic cavity sizes that are defined by number of glucose units and two different rims, a wider rim (named head, H) bearing only secondary hydroxyl groups and a narrower rim (named tail, T) possessing only primary hydroxyl groups.[11] The presence of different numbers of hydroxyl groups

Surfactant and Colloid Group, Department of Chemistry, The University of Hull, Hull, HU6 7RX, UK. E-mail: V.N.Paunov@hull.ac.uk; Fax: +44 (0)1482 466410; Tel: +44 (0) 1482 465660

† Electronic supplementary information (ESI) available. See DOI: 10.1039/c3ta12108a

has a profound influence on the physical properties of CDs. Since the threading of CDs along the polymer chain is reported to be assisted by hydrogen bonding, the way CD rims face each other along the polymeric chain length is expected to influence the morphology of the supramolecular structure.[12] The isomers representing possible ways CD rims may face each other along the polymer chain have been reported as TT, HH and HT.[13] One therefore expects different types of CDs to have preferred orientation along the polymeric chain which in turn determines the size, crystallinity, and morphology of the supramolecular structure and other physical properties such as aggregation behaviour.

Several research groups have reported crystalline or soluble pseudopolyrotaxanes[14] from CD and linear polymer molecules. Harada and Kamachi[15] reported the first example of an IC formed *via* the self-assembly of α-CD and poly(ethylene glycol) (PEG) and since then, other researchers have reported results obtained by using different types of CDs and polymers.[9,16–19] Although the formation of CD–polymer ICs and their shape[20] have already been reported before, the effect of the CD type on the aggregation behaviour of these pseudopolyrotaxanes in aqueous solution has not been fully addressed.

Herein, we report different aggregation behaviour of pseudorotaxanes between a linear alkane, *n*-tetradecane, and α-CD and β-CD in aqueous solutions. These ICs were formed spontaneously at the oil–water (o/w) interface by a self-assembly process without stirring or agitation. They were also alternatively formed upon dispersing *n*-tetradecane in CD aqueous solution by homogenization. Such ICs were found to form microcrystals which are very effective in stabilisation of Pickering types of emulsions (*i.e.* solid stabilised emulsions). Therefore, they can be useful in areas such as drug delivery and in a wide range of emulsion technologies where they can be used to spontaneously form Pickering emulsions. We discovered that the rate of formation of these ICs at the o/w interface and their microcrystal growth and morphology are determined by the type of CD used. We have also observed that the shapes and size of the IC structures formed were dependent on the type of CD used.

Experimental

Materials

Water was purified by passing through a reverse osmosis unit and then a Milli-Q® reagent water system (resistivity 18 MΩ cm). α-CD, β-CD and γ-CD were purchased from Sigma and used without any further purification. Tetradecane (99%) and hexadecane (99%, both from Sigma) were passed twice through chromatographic alumina (0.063–0.200 nm, Merck) in order to remove polar impurities before use. NaOH (99%) was purchased from Fisher Scientific. Urea (99%) was purchased from Sigma and used without further purification. Nile Red (98%) from Sigma was used as received.

Characterisation methods

Air–water and oil–water interfacial tension measurements. A series of standard aqueous solutions of CDs were prepared in Milli-Q water and then equilibrated at 25 °C in a thermostatic water bath. Their air–water surface tensions were measured using a pendant drop method (Krüss Drop shape analyser DSA 10, Hamburg, Germany). Measurements were performed by producing a pendant drop (top-to-bottom) of aqueous solutions from a Hamilton syringe (needle diameter 1.832 mm), recording the drop shape with a CCD camera and then fitting the Young–Laplace equation to the drop image. The oil–water interfacial tension was performed by producing a pendant drop (bottom-to-top) of oil from a J-shaped syringe needle (needle diameter 1.500 mm) into a bath of CD aqueous solutions in a quartz cuvette (24 mm × 24 mm × 21 mm). The drop images were recorded with a CCD camera and the interfacial tension calculated by fitting the drop profile with the numerical solution of the Young–Laplace equation. Both the surface tension and the interfacial tension were measured shortly after the droplet was produced at 25 °C and the system was calibrated by measuring the surface tension of Milli-Q-water 72.00 ± 0.01 mN m^{-1}. Some results were obtained using a Kruss Digital Tensiometer K10 (A Kruss Hamburg Germany) by applying the Du Nouy ring method. The temperature of the sample was maintained at a constant value (25 ± 1 °C) by a circulatory water thermostat from IKA. To measure the surface tension, each sample was placed in a glass container, placed in a measurement zone and left for 20 minutes to attain equilibrium.

Optical microscopy. The morphology and the crystalline properties of the CD–tetradecane IC microrods were examined using an Olympus BX 51 optical microscope (Olympus, Japan) with phase contrast objectives and the images were captured with a DP 70 Olympus digital camera (Japan) using Image Pro Plus® software (USA).

Scanning electron microscopy (SEM). The IC crystalline sample dispersed in Milli-Q water was deposited on a (~1 cm × 1 cm) microscope glass slide and then air dried. The sample was then gold sputter-coated under high vacuum to avoid charge accumulation during analysis. The gold coated sample was then mounted on a SEM sample stub and viewed with a Zeiss EVO 60 SEM with the LaB_6 filament.

Transmission electron microscopy (TEM). The sample was negatively stained to enhance imaging contrast by mixing 5 μL of the CD–tetradecane IC microrod dispersion in Milli-Q water with 5 μL of 2% aqueous solution of uranyl acetate. The sample was then washed in water, deposited and dried at ambient temperature on a TEM copper grid, and then viewed with a JEOL 2010 TEM (Japan) operating at 80 kV. Lanthanum hexaboride (LaB_6) crystals were used as the electron source. TEM images were captured with a Gatan US4000 digital camera.

Fourier transform infrared spectroscopy (FT-IR). Infrared spectra were obtained for the raw materials and the products for the purpose of comparison by using a PerkinElmer FTIR spectrometer (USA). The spectra were obtained by FT-IR-Attenuated Total Reflectance (ATR) using a diamond crystal. The IR background was obtained by scanning a clean ATR-diamond crystal surface. The dry solid samples were then placed to cover the diamond crystal area and clamped to the surface by applying pressure to ensure a good contact between the sample and the diamond crystal surface. The scans were then carried out at a resolution of 1.0 cm^{-1} (from 4000 to 650 cm^{-1}). The FT-IR

spectrum of pure liquid tetradecane was obtained by placing liquid tetradecane between two NaCl solid discs which were then secured in a holder before running the spectrum from 4000 cm^{-1} to 600 cm^{-1}. The background was set using air with a resolution of 1.0 cm^{-1}.

Carbon elemental analysis. The stoichiometry of the CD–tetradecane inclusion complex (number of CD molecules per tetradecane molecule) was estimated by elemental analysis (C) which was carried out using a Carlo Erba EA 1108 CHN Fisons Instrument. Helium gas with a flow rate of 140 mL min^{-1} was used as a carrier gas while pure oxygen flowing at 20 mL min^{-1} was used for combustion.

Results and discussion

Self-assembly of tetradecane–CD inclusion complexes at the o/w interface

We observed in real time the formation of microcrystals of IC (poly(pseudo) rotaxanes) due to threading of CD molecules along the tetradecane molecules at the o/w interface. The schematic of our setup used to monitor the intensity of light transmitted through the oil droplet in aqueous solution onto a CCD camera is shown in Fig. 1a. Self-assembly and threading of CDs along a single tetradecane molecule at the o/w interface form microparticles which grow and remain adsorbed at the interface which leads to scattering of light. This manifests itself as clouding at the o/w interface as visually observed in Fig. 1b. Oil droplet images of varying light intensities were captured at different time intervals to show the formation of IC microcrystals due to the CD threading and assembly at the o/w interface. From these experiments, we discovered that threading of CD along the tetradecane molecule and the microcrystal formation is dependent on the CD used and the size of its hydrophobic cavity.

Air/water surface tension in the presence of CD

The air/water surface tension as a function of the CD concentration was measured using a Drop Shape Analyser (DSA). As shown in Fig. 1c, all non-modified CDs were non-surface active at the air/water interface. In contrast, methyl-β-CD showed measurable surface activity.

Oil–water interfacial tension in the presence of CDs in the aqueous phase

CDs are known to form host–guest inclusion complexes by embedding either the entire hydrophobic guest molecule or only its hydrophobic part in their hydrophobic cavities.[5,6] This process could potentially create pseudo surfactant structures between tetradecane and CDs that can self-organise at the o/w interface with the CDs acting as head groups (hydrophilic) and the remaining (non-included) part of the tetradecane hydrocarbon chain as the tail (hydrophobic). The self-organisation of these pseudo surfactants formed between tetradecane and CDs at the o/w interface was monitored by interfacial tension measurement using a sessile oil droplet sitting on the tip of the J-shaped syringe needle which allowed oil drop to be produced in a controllable way into the CD aqueous phase.

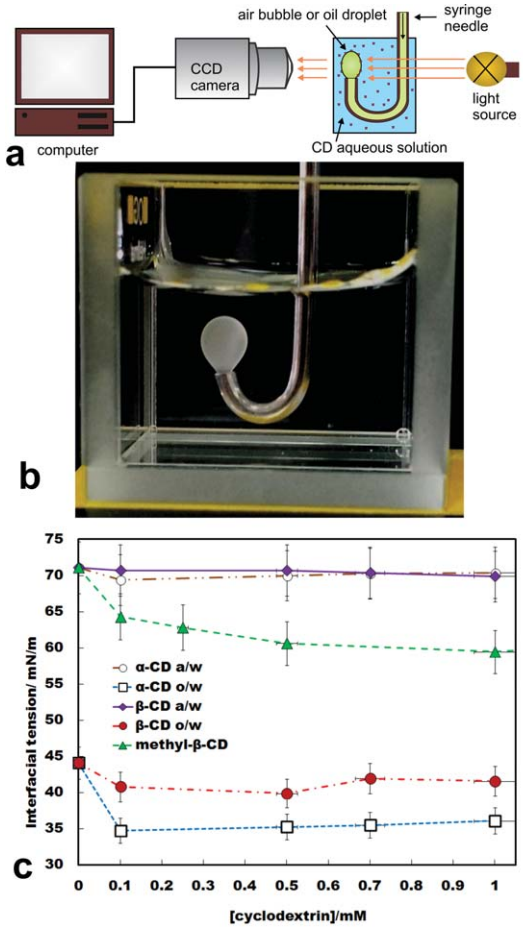

Fig. 1 (a) Schematics of the set up for monitoring the surface tension and the formation of ICs at the tetradecane–water interface in the presence of various types of cyclodextrins. (b) Image of a tetradecane drop in 10 mM aqueous solution of α-CD in a quartz cuvette. Note the clouding caused by α-CD–tetradecane IC microcrystals formed at the o/w interface. (c) Effect of the α-CD and β-CD concentrations on the air/water surface tension and the tetradecane–water interfacial tension. We also present the effect of the methyl-β-CD concentration on the air/water surface tension.

Fig. 1c shows that the presence of CDs in the aqueous phase leads to a decrease in interfacial tension compared to its value in the absence of CDs. This observation suggested that the surface active material is indeed formed at the o/w interface in the presence of CDs in the aqueous solution. It was observed that at the same CD concentration in the aqueous phase, the o/w interfacial tension decreased more in the presence of α-CD compared to β-CD. In addition, we discovered that microrod-like crystals were formed at high CD concentration (10 mM). This observation suggested that threading of more than one CD molecules along a single tetradecane molecule is likely to take place at high CD concentration.

The series of images presented in Fig. 2A demonstrate that the formation of IC microrods at the o/w surface due to α-CD threading along the tetradecane is faster compared to the same phenomenon with β-CD at the same concentration (10 mM) in the aqueous phase. For instance, a tetradecane drop produced in a bath of 10 mM of α-CD aqueous solution was completely covered with the microcrystals after 12 minutes, after which it

detached from the capillary tip without regaining spherical shape.

In contrast, the tetradecane drop produced in a bath of 10 mM β-CD aqueous solution remained transparent and attached to the capillary tip after 1 h of exposure (see Fig. 2B). A sample of the α-CD–tetradecane IC microcrystals was collected with a Pasteur pipette from the aqueous phase near the o/w interface and deposited directly onto a microscope glass slide. Optical microscopy observation, as shown in Fig. 2D, revealed microrod-like structures. This suggests that α-CD–tetradecane ICs are likely to involve threading of more than one CD along the length of the tetradecane molecule at the o/w interface, which allows the tetradecane molecule in the IC to reduce its exposure to the aqueous phase and form nanorods and microrods. The inherent anisotropy of the IC leads to formation of anisotropic microparticles. The growth of nanorods into microrods is supported by directional hydrogen bond networking of threaded CD hydroxyl groups on neighbouring nanorods. The growth of these nanorods into microrods and their self-assembly at the o/w interface around the oil droplet represent a different mechanism for stabilisation of o/w emulsions which starts with molecular adsorption of CD at the o/w interface but ends up as a Pickering emulsion due to the retention of the formed IC microcrystals at the interface. Upon withdrawing tetradecane from the drop, the area of the o/w interface remained approximately the same but the droplet maintained its deformed shape. This indicates that the adsorbed IC microcrystals stop the o/w interface from contracting. As seen in Fig. 2C, the droplet regained its original shape after "re-inflating" with tetradecane. This also suggests that free oil molecules in the drop are surrounded by a dense layer of entangled CD–tetradecane microcrystals. The stability of these microrods at the o/w interface is possibly enhanced by a strong hydrogen bonding network from neighbouring microrods. We also produced a completely detached oil drop stabilised by α-CD–tetradecane IC microrods which was stable and retained its original shape in α-CD aqueous solutions. This indicates the ability of the α-CD–oil microrods to stabilize the oil droplets in water as shown in Fig. 2A.

Preparation of dispersed CD–tetradecane IC microrods

We prepared these microrods by dispersing 10 μL of tetradecane in 10 mL of aqueous solutions of either α-CD or β-CD at a concentration of 10 mM. This was achieved by homogenizing the two liquid phases at 11 000 rpm for 20 seconds with an Ultra Turrax. The morphology of CD–tetradecane microrods (α- and β-) was studied by using SEM imaging which showed different shapes and sizes of these microcrystals dependent on the type of the CD used. We observed lamella-like sheets and microrods from α-CD–tetradecane ICs as shown in Fig. 3I-a and b. In addition, the microrods from α-CD–tetradecane had a very high aspect ratio (see Fig. 3I-d). Observation over a large number of SEM images suggests that these long microrods stack together to produce the lamella-like sheets.

The stacking of α-CD–tetradecane IC microrods is indicated by red arrows in Fig. 3I-c. The staking of the α-CD–tetradecane microrods could be the result of directional hydrogen bonding between neighbouring hydroxyl groups of CD molecules threaded on parallel tetradecane molecules. The long microrods were characterised by different cross-sectional areas as shown in Fig. 3I-e and f. We also present TEM images of the same α-CD–tetradecane IC microrods in the ESI (Fig. S1†). Contrary to the

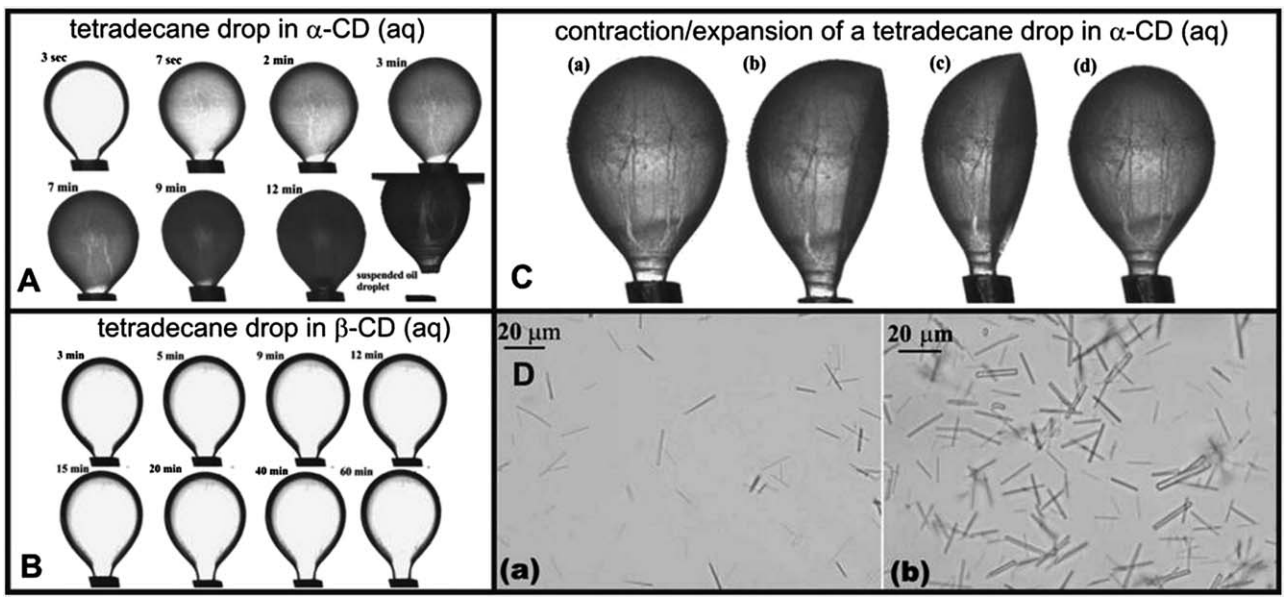

Fig. 2 (A) Optical images showing the formation of α-CD–tetradecane ICs at the o/w interface as a function of time. Note that the oil drop gets completely coated with IC microcrystals while exposed to the α-CD solution and retains its shape after detaching from the needle tip. (B) Optical images of a tetradecane droplet in 10 mM β-CD aqueous solution captured at different times. This illustrates that compared to α-CD–tetradecane ICs, the formation of β-CD–tetradecane ICs goes at a lower rate. (C) Optical images illustrating the effect of contraction/expansion of the tetradecane drop densely coated with α-CD–tetradecane IC microcrystals on the drop shape. The images (b) and (c) indicate that the droplet remains deformed after withdrawing the core oil into the syringe; (d) the droplet goes back to its original shape after infusion with tetradecane; (D) optical micrographs of α-CD IC microcrystals collected from the area close to the o/w droplet interface – see (C).

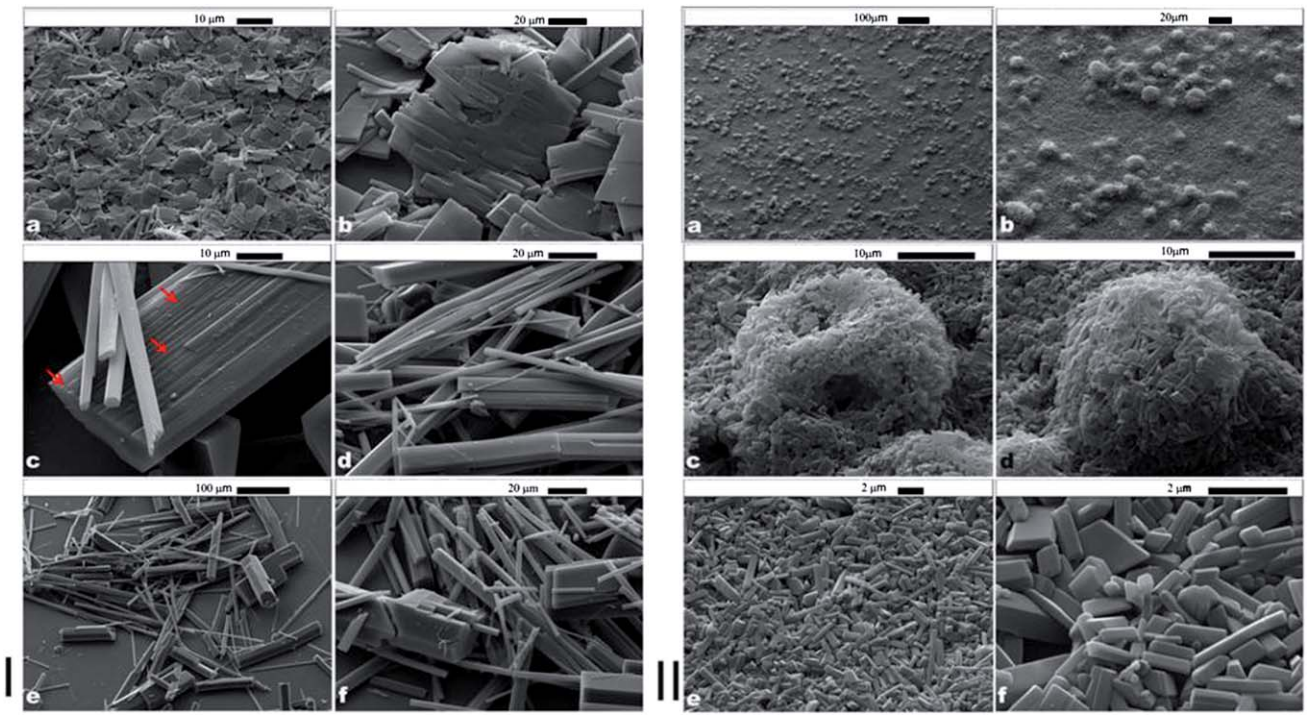

Fig. 3 (I) α-CD–tetradecane ICs: (a) and (b) lamella plate structures; (c) lamella sheets formed from stacking of long microrods shown by red arrows; (d) long microrods responsible for forming lamella plates; (e) and (f) some IC microrods showing different cross-sectional areas. (II) β-CD–tetradecane ICs: (a) to (d) spherical structures formed by heating up of β-CD–tetradecane ICs. (e) and (f) Short microrods formed β-CD–tetradecane ICs.

microrods from ICs with α-CD, the analogous IC microrods from β-CD were shorter and did not form the lamella structures like the α-CD–tetradecane IC microrods (see Fig. 3II-e and f). The aggregation behaviour of these ICs depends on the type of CD used. While the long α-CD–tetradecane IC microrods favour stacking to give lamella plates, the shorter β-CD–tetradecane IC microrods additionally aggregate forming spherical clusters as shown in Fig. 3II-a and d. One possible reason for the latter clustering, however, could be the presence of residual oil drops.

The difference in structure and aggregation behaviour between α-CD and β-CD–tetradecane IC microrods could be explained by considering the solubility of the 3 common CDs (α, β and γ). It is well known that γ-CD, which is the largest of the three, is the most soluble while β-CD, which is in the intermediate, is the least soluble in water. These differences in the solubility of the CDs are related to the way the CD glucose units are geometrically aligned with each other. It has been proposed that in the β-CD molecule, all the 7 glucose units lie in the same plane. In this arrangement, all the glucose primary hydroxyl groups at the CD narrower end are able to form hydrogen bonds with each other. At the same time, all the secondary hydroxyl groups at the wider CD opening form hydrogen bonds with each other. The hydrogen bonding below and above the ring leads to secondary belts which increases the rigidity of the β-CD and hence causes low solubility.[21] In contrast, α-CD and γ-CD do not have secondary belts hence their structures are flexible and are therefore very soluble due to the availability of free hydroxyl groups. It has been reported that that hydrogen bonding assists the threading of CD along the chain of the guest molecule.[19] Using the above reasoning, since α-CD molecules have free hydroxyl groups the threading over tetradecane can occur faster than that with β-CD as confirmed by our results.

Free hydroxyl groups can also participate in hydrogen bonding with neighbouring microrods to form lamella plates and longer rods. β-CD has a more limited ability to form hydrogen bonds compared to α-CD hence the process of threading over tetradecane is slower and leads to shorter microcrystals than the ones with α-CD.

We performed control experiments by stirring 10 mL of 10 mM of aqueous solution of α-CD or β-CD without tetradecane at the same homogenisation rate and duration to check if any precipitate will be formed at room temperature. These experiments did not produce any precipitate or clouding of the solution. We therefore concluded that the micro-rod structures were not formed due to crystallisation of CDs because the concentrations of both CD aqueous solutions were lower than their maximum solubility limit at room temperature (150 mM for α-CD and 16.3 mM for β-CD). We observed the dry powder of the pure CDs with an optical microscope to see if similar aggregations were present. As shown in Fig. 4, the powder of pure CDs gave different structures from the microcrystals obtained in the presence of tetradecane which is an indication that threading of CDs on the tetradecane plays a big role in the formation and aggregation of these microrods.

Crystallinity of the CD–tetradecane IC microrods

The precipitated α-CD–tetradecane IC material had the appearance of a white and shiny solid whereas the β-CD–tetradecane IC solid was "powdery", white and non-shiny. The difference in the crystallinity of α-CD and β-CD ICs with

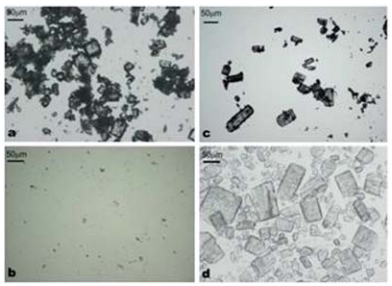

Fig. 4 Microscope optical micrographs of: (a) pure α-CD powder; (b) saturated aqueous solution of α-CD; (c) pure β-CD powder; (d) β-CD crystals produced from supersaturated solution.

tetradecane was confirmed by optical microscopy in cross-polarised light. Small samples of the precipitates were withdrawn with a Pasteur pipette, then deposited directly on a clean microscope glass slide and analysed. The α-CD–tetradecane IC microrods showed some birefringence when observed under the cross-polarised light optical microscopy. However, most of the rods exhibited somehow Janus characteristics with one shiny end of the rods while the other end was less or not shiny at all (see Fig. 5b and d). This suggests that the microrods could consist of crystalline and amorphous regions. In contrast, microrods from β-CD samples did not show any birefringence.

This suggested that the mechanisms of packing cyclodextrin molecules to form the micro-rods were different. The free hydroxyl groups on α-CD promote well-ordered microrods as a result of hydrogen bonding leading to the crystalline structure. The more limited hydrogen bonding in β-CD is less likely to produce long ordered microrods thus leading to smaller IC microcrystals.

Factors affecting the formation of CD–tetradecane microrods and their structures

CD hydrophobic cavity diameter. The effect of the CD hydrophobic cavity size was investigated by dispersing 10 μL of tetradecane in 10 mL of 10 mM aqueous solutions of three different CDs (α, β and γ) and homogenized with an Ultra Turrax. We observed that the γ-CD sample became clear throughout the solution in a short time. On the other hand, the α-CD sample gave a precipitate at the bottom of the sample tube and a clear solution on top in less than 30 minutes. The β-CD sample in contrast remained turbid throughout the solution even after three days (see Fig. S2† in ESI). From these results, we conclude that the cavity of the hydrophobic cavity plays an important role in the formation of CD–tetradecane microrods. The γ-CD hydrophobic cavity is probably too wide to hold on the tetradecane chain, therefore the γ-CD can easily detach from the tetradecane chain leading to poor stability of the microrods. On the other hand, our estimate shows that the γ-CD internal cavity is too small to hold two packed molecules of tetradecane in their stretched state (see ESI and Scheme 1d).

Effect of temperature on the α-CD–tetradecane microrods. α-CD–tetradecane IC microrods were prepared by dispersing 10 μL of tetradecane in 10 mL of 10 mM α-CD. The aqueous sample of these micro-rods was then split into 4 sample tubes and each tube was then immersed and heated for 15 minutes in a water bath preset at a particular temperature (30, 50, 65 and 85 °C) and the change in the morphologies was observed using transmitted light microscopy. As expected, the micro-rods were disintegrated as the temperature was increased due to the breakdown of the hydrogen bonding as well as de-threading. Above 80 °C, roughly in the range 81–85 °C the rods were completely dissolved. However, after the dissolution followed by cooling, some self-assembly of micro-rods into spherical structures on the microscope glass slide was observed. Fig. 6a shows the build up of spherical structures on a microscope glass slide during the cooling of the resultant aqueous α-CD solution from α-CD microrods dissolved at 85 °C. The micrograph was taken 5 minutes after depositing the hot α-CD–tetradecane aqueous solution. As seen in Fig. 6b, larger spherical structures were obtained 15 minutes later in the process of

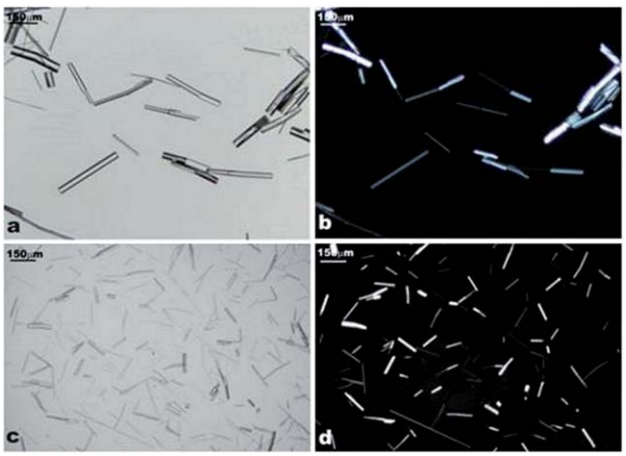

Fig. 5 (a) and (c) Optical microscope images of α-CD–tetradecane IC microrods; (b) and (d) optical images of the same samples in cross-polarised light.

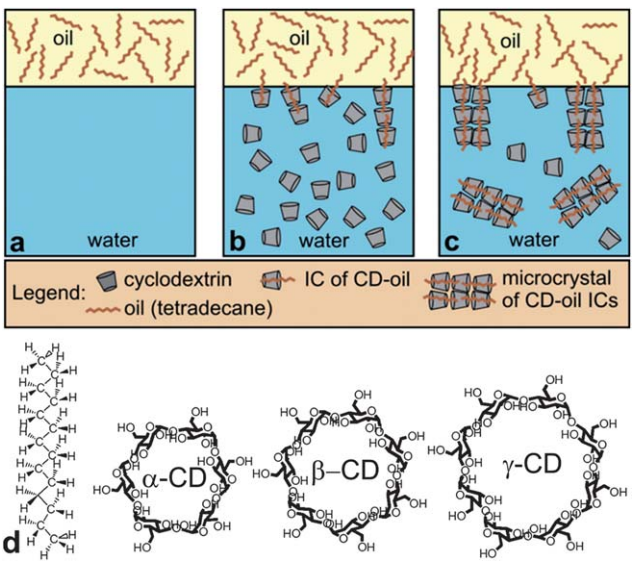

Scheme 1 Influence of α-CD and β-CD concentrations on air–water surface tension and tetradecane–water interfacial tension. (d) Molecular structures of tetradecane, α-CD, β-CD and γ-CD.

cooling as indicated by red arrows on the micrographs. This thermo responsive self-assembly of α-CD microrods from lamella plates to spherical structures opens up a new avenue for creating novel materials with potential applications in encapsulation of active components using α-CD.

Effect of pH on the formation of CD–tetradecane IC microcrystals. The effect of pH was investigated by preparing α-CD–tetradecane microrods by dispersing 10 μL of tetradecane in 10 mL of 10 mM of α-CD aqueous solutions at three different pH values (1.98, 7.16 and 11.60). The volume fraction of the precipitate was measured after 24 h and 7 days, respectively following the initial homogenisation. As shown in Fig. 7a, micro-rods were formed at all three different values of pH but their formation was less favoured at high pH (11.60). As seen in Fig. 7a, after 24 h, the sample at pH 11.60 was still turbid and had the smallest volume fraction of the precipitated micro-rods. This observation could be attributed to the ionization of the α-CD hydroxyl groups by deprotonisation at high pH. Hydrogen bonding enhances the threading of several CDs along the chain of the guest molecule but in contrast, a negatively charged CD molecule already threaded would repel electrostatically another incoming ionized CD molecule. This is expected to lead to the formation of fewer microrods and furthermore, their electrostatic repulsion would keep them suspended in aqueous solution. This leads to stabilisation of the suspension against precipitation and therefore explains why the sample at pH 11.60 was turbid even after 24 hours compared to the samples at lower pH.

Since the neutral threaded CDs (pH 7.16) have no electrostatic repulsion and the microrods attract each other with hydrogen bonds and van der Waals attraction among them, they would therefore aggregate and sediment due to gravity.

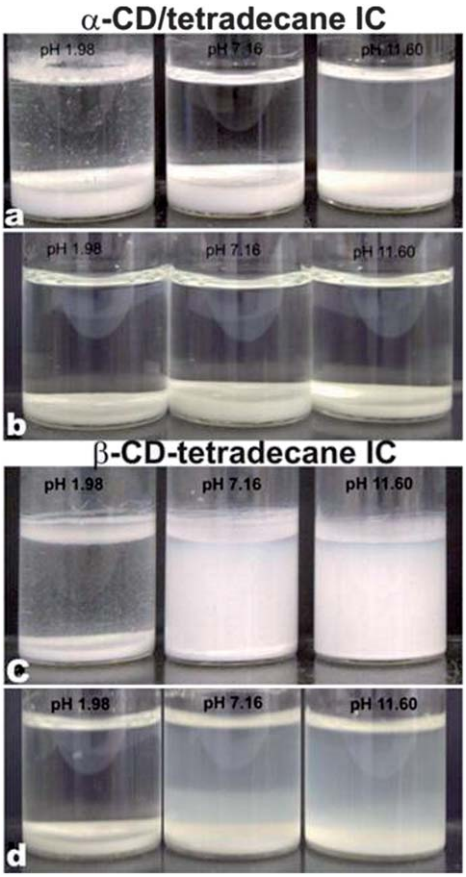

Fig. 7 Influence of pH of the aqueous solution on the formation of microcrystals of α-CD–tetradecane ICs (a and b) and β-CD–tetradecane ICs (c and d): images (a) and (c) were captured 24 hours after the initial mixing of CD and tetradecane, while images (b) and (d) were captured after 7 days.

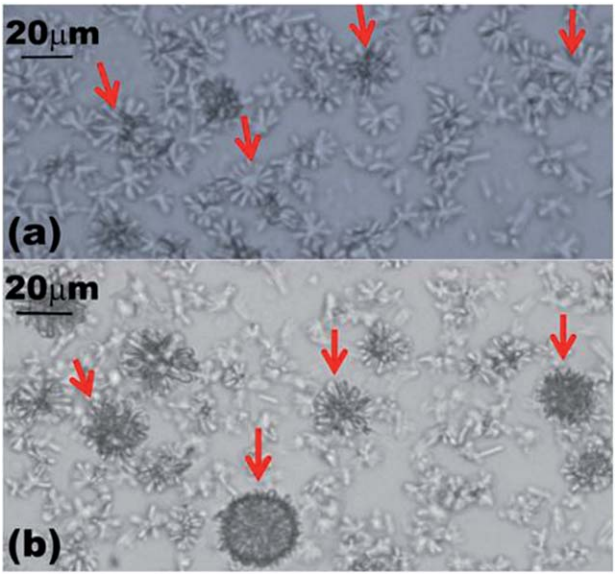

Fig. 6 Optical images showing the formation of spherical structures by α-CD–tetradecane ICs after dissolving the microrods by heating them at 85 °C before cooling to room temperature. (a) Optical micrographs showing the process of forming spherical structures 5 minutes after the aqueous solution was deposited on the microscope glass slide from a hot bath. (b) The same sample 15 minutes later on the microscope slide.

However, when the precipitate volume fractions were analysed after 7 days, the volume fraction of the sample at low pH (1.98) had decreased more than any other samples and had the smallest volume fraction. This suggests that the α-CD microrods were not stable for a long time at low pH. This instability could be due to dissolution and de-threading of the microrods as well as hydrolysis of CDs. The microrods prepared at pH (7.16) appeared to be the most stable which indicates that uninterrupted hydrogen bonding is one of the important parameters for the formation of CD–tetradecane microrods.

In contrast, β-CD containing samples at pH 7.16 and 11.60 were turbid after 24 hours as well as after seven days. These samples showed little precipitation compared to the sample prepared at pH 1.98 which also exhibited fast precipitation. The difference in the rate of formation of the β-CD–tetradecane IC microrods and their precipitation could be attributed to the secondary belts due to intrahydrogen bonding above and below the β-CD ring. This secondary ring formations reduce the ability of β-CD hydroxyl groups to form inter-hydrogen bonding with incoming β-CD molecules on the tetradecane molecule. This therefore impedes the threading process, the growth of the microrods and their precipitation. We propose that low pH (1.98) disrupts the β-CD secondary belt hydrogen bonding. The

free β-CD hydroxyls then participate in cooperative hydrogen bonding with hydroxyl groups on neighbouring β-CD to enhance the threading of other incoming CD molecules along the tetradecane chain. This leads to enhanced formation of microrods and their precipitation as shown in Fig. 7c. At pH 7.16, the secondary belts are uninterrupted and hence the threading and precipitation processes are slow. Fig. 7c and d show that the sample at pH 11.60 yielded the smallest volume fraction of the precipitate. This low yield was attributed to a combination of the slow threading process due to the secondary belts and the electrostatic repulsion between negatively charged β-CD ions at high pH (11.60).

We discovered that α-CD tetradecane microrods formed favourably at neutral pH (7.16) where the hydroxyl groups are not disturbed and fully participate in cooperative hydrogen bonding for enhanced threading and growth of the IC microrods.

In contrast, β-CD–tetradecane IC microrods were preferably formed at low pH (1.98) which was necessary to disrupt the secondary belts and free β-CD hydroxyl groups to participate in inter-cooperative hydrogen bonding to increase the rate of threading and subsequent precipitation. The rate of β-CD threading and subsequent precipitation was slow at both the o/w interface and in the bulk compared to the results with α-CD. In the ESI (Fig. S3 and S4†) we present in more detail the optical microscopy images of the morphology changes in the microcrystals of α-CD–tetradecane and β-CD–tetradecane ICs formed under different pH over the period of 7 days. Our observations show significant differences in the rate of growth of the IC microcrystals.

FT-IR spectroscopy. We investigated how the vibration frequencies of the pure CDs were affected by threading of CDs along tetradecane molecules in aqueous solutions at different pH values by comparing their FT-IR spectra. We also compared the vibration spectra of the microrods from α-CD–tetradecane ICs with those of β-CD–tetradecane IC microrods since they showed different aggregation behaviour and precipitation rates. Precipitates were withdrawn with Pasteur pipettes and then transferred to Ependoff sample tubes. The samples were then washed by adding Milli-Q-water followed by gravity sedimentation and subsequently the supernatant was carefully withdrawn with a Pasteur pipette to remove any free CDs. This washing procedure was repeated three times before the samples were finally air-dried. We used the FT-IR ATR diamond crystal instead of the KBr method to minimise destroying the microrods which would otherwise introduce free CDs in the mixture due to grinding.

FT-IR spectra for α-CD–tetradecane IC microrods. The vibration frequency patterns from α-CD–tetradecane IC microrods prepared in aqueous solutions at three different pH values were all the same. However, the spectra of the α-CD–tetradecane IC microrods were different from the vibration spectrum of the pure α-CD. All microrods showed high absorbance compared to the pure α-CD and the band peaks were much more resolved. The difference in the vibration patterns was noticeable in the fingerprint region as shown in the expanded parts labelled (a and b) of the spectra. As seen in Fig. 8a and b, the two bands at 1000 and 1058 cm^{-1} were present in the pure α-CD spectrum but these peaks were absent in the spectra of all the α-CD–tetradecane microrods. In addition, a new band peak at 1098 cm^{-1} was observed for the microrods while it was absent in the pure α-CD vibrational spectrum. The differences in the vibrational frequency patterns in the fingerprint region suggest that CDs in the microrods were in a chemical environment that was different from the CDs in their pure form. From this experiment, it was observed that peaks associated with the vibrations from tetradecane molecules were suppressed. The microrod vibrational spectra have two band shoulders at 2890 and 1452 cm^{-1} which were absent in pure α-CD. These peaks could be attributed to symmetric C–H stretching and C–H bending from tetradecane. This suggests that the tetradecane molecules were buried in the CD cavities and their vibrational motions were restricted since they were forced to adopt extended conformation by the CD cavities. We have also found that the band peak around 3300 cm^{-1} which was attributed to O–H stretching was shifted to a lower frequency in the microrods, probably due to the presence of strong hydrogen bonding. The latter stretches the O–H bond length therefore leading to lower vibrational frequencies.[22]

Effect of urea on the CD–tetradecane microcrystal formation. A chaotropic agent is a solute that disrupts the chemical structures of macromolecules that are stabilized by non-covalent forces such as hydrogen bonds and the hydrophobic effect. Urea at high concentration (8 M) is one example of a chaotropic agent that has been employed to unfold protein structures.[15] α-CD and β-CD microrods were formed due to a hydrophobic effect, van der Waals forces and hydrogen bonding. We investigated the effect of urea on the structure of the α-CD–tetradecane microrods in aqueous solutions of urea at three different concentrations (0.5 M, 1 M and 5 M). The change in the morphology and size of the microrods with time was monitored using an optical microscope. We observed that α-CD–tetradecane microrods prepared at low urea concentrations (0.5 M and 1 M) increased in length with time (Fig. 10) while those prepared at 5 M urea were completely degraded. Fig. 11 shows the increase in the microrod length through end-to-end connections. Small microrods were connected to each other by joining their ends due to directional hydrogen bonding from neighbouring terminal CD hydroxyl groups. The end-to-end connections between initially formed microrods are marked with red circles in Fig. 11. The effect of urea on β-CD structures was investigated by preparing the microrods by dispersing tetradecane in urea in aqueous solutions of urea at two different concentrations (0.1 M and 1 M). Contrary to the increase in length we observed in α-CD–tetradecane structures, the spherical structures obtained from β-CD–tetradecane were degraded at these concentrations with time (see Fig. S5† in the ESI for more details). From these experiments we can conclude that α-CD structures were formed and held by stronger hydrogen bonding compared to β-CD–tetradecane IC crystalline structures.

The band peaks in the tetradecane spectrum (Fig. 9) were assigned as follows: band peaks at 2922.77 cm^{-1} and 2853.19 cm^{-1} were attributed to C–H asymmetric and symmetric

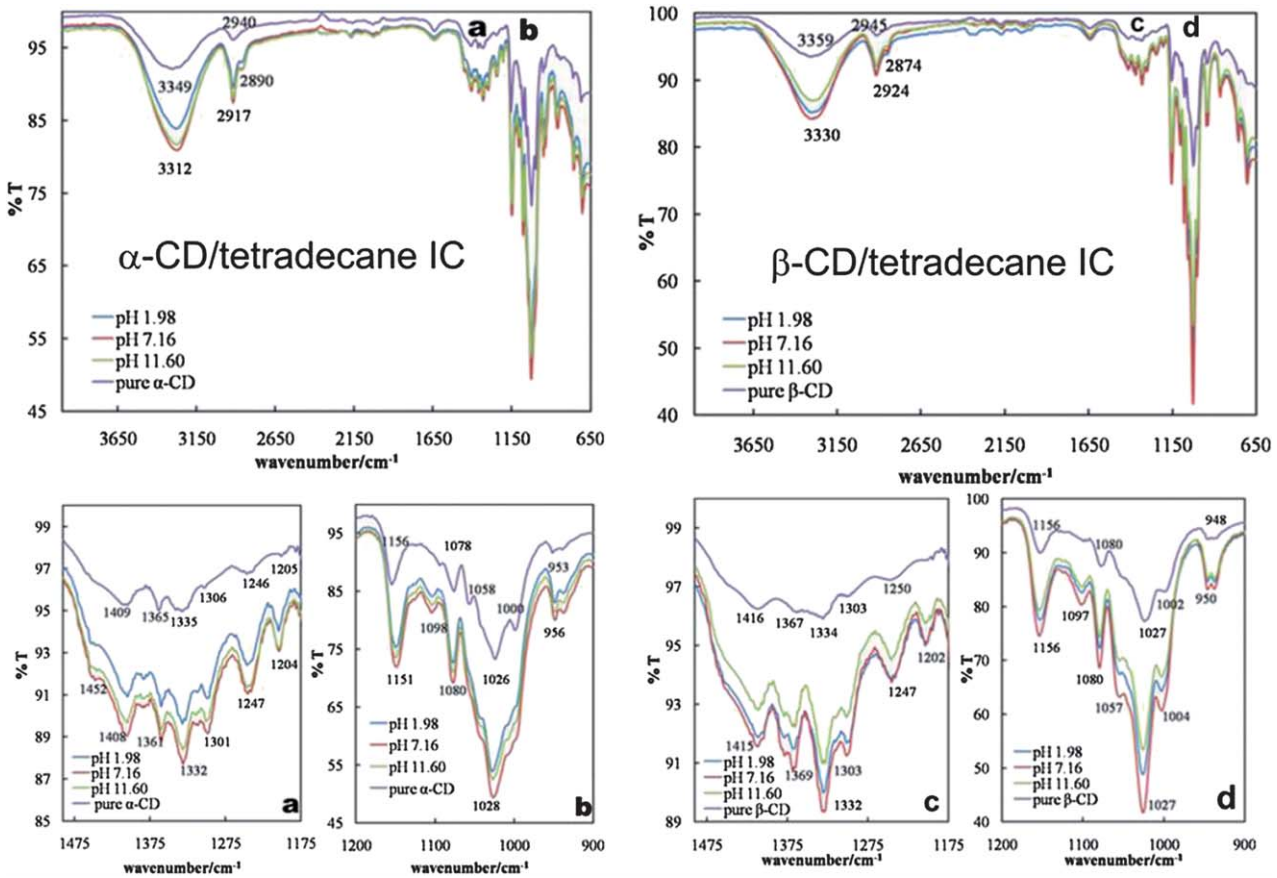

Fig. 8 LHS images: FT-IR spectra of pure α-CD and α-CD–tetradecane ICs prepared in aqueous solutions at different pH. An expanded region labelled (a) and (b) in the main spectra is shown below. RHS images: FT-IR spectra of pure β-CD and β-CD–tetradecane ICs prepared in aqueous solutions at different pH. An expanded region labelled (c) and (d) in the main spectra is shown below.

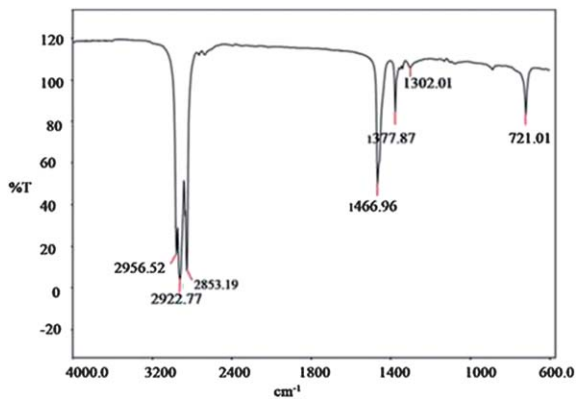

Fig. 9 FT-IR spectrum of pure tetradecane.

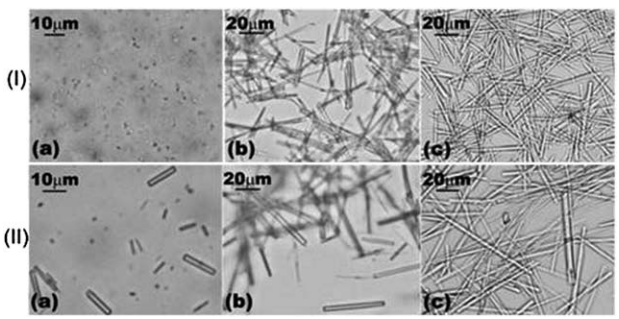

Fig. 10 Optical micrographs showing the effect of urea concentration on the size of α-CD–tetradecane IC microrods as a function of time. Row I: in 0.5 M urea (a) immediately after dispersion; (b) after 24 hours; and (c) after 3 days. Row II: in 1 M urea (a) immediately after dispersion; (b) after 24 hours; and (c) after 3 days.

stretching respectively. A band peak at 1466.96 cm^{-1} is attributed to the C–H bending. The peaks are consistent with ref. 23.

Effect of the oil type on the IC formation. We investigated the effect of chain length of the guest molecule by using *n*-hexane and *n*-hexadecane. Each oil was dispersed in 10 mL of 10 mM of α-CD and β-CD aqueous solution under the same homogenization speed and time as for tetradecane. *n*-Hexane did not yield any microrods with either α-CD or β-CD. This could be because the whole molecule of *n*-hexane was encapsulated in the hydrophobic cavities of the CDs. However, we obtained microrods with α-CD with *n*-hexadecane which grow both by length and diameter with time as shown in Fig. 12a and b. On the other hand, β-CD-hexadecane gave spherical structures and these structures appeared to break down in the solution after 3 days. The results were similar to those from

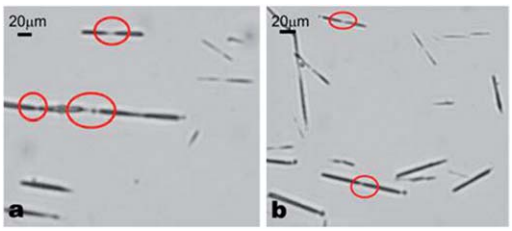

Fig. 11 α-CD–tetradecane ICs prepared in 1 M urea solution showing some end-to-end joining which leads to their elongation with time. The end-to-end connections are highlighted by red circles.

tetradecane. The α-CD microrods exhibited some birefringence (see insets in Fig. 12a) while the β-CD structures did not.

The ability of β-CD–oil structures to serve as potential microencapsulating vehicles was probed by doping 5 mL of tetradecane with 2.5 μL of 2×10^{-4} M Nile Red in acetone. 10 μL of the Nile Red doped tetradecane was then dispersed by homogenization in 10 mL of 10 mM β-CD aqueous solution. As it can be seen in Fig. 13, most of the Nile Red is concentrated in the β-CD–tetradecane structures compared to the bulk. This showed that these structures can be useful in encapsulating oil soluble active components.

Stoichiometry of CD–tetradecane inclusion complexes. We have studied the ratio of the cyclodextrin-to-tetradecane in the inclusion complex in an attempt to characterise the way this complex is formed.

We employed elemental analysis of our samples of α-CD, β-CD (crystals) and the inclusion complexes of these materials with tetradecane. The results for the carbon content in the samples presented here allowed us to estimate the number of α-CD and β-CD molecules threaded per molecule of tetradecane. Our data show the following approximate stoichiometries of these complexes, $\alpha\text{-CD}_{6.8}\text{TD}_1$ and $\beta\text{-CD}_{5.7}\text{TD}_1$, respectively. Our results suggest that the stoichiometry is independent of the volume of the oil, as the same results were obtained by using two different amounts of TD (10 μL and 20 μL) with the same amounts of 10 mM α-CD and β-CD solution. The maximum theoretical number of CDs per stretched length of TD with 109° between C–C–C bonds was estimated to be 5.6 for both α-CD and β-CD assuming close packing of the threaded CDs. We propose that the CD–tetradecane inclusion complexes are formed by TD molecules along CD nanotubes with some additional voids with included water molecules.

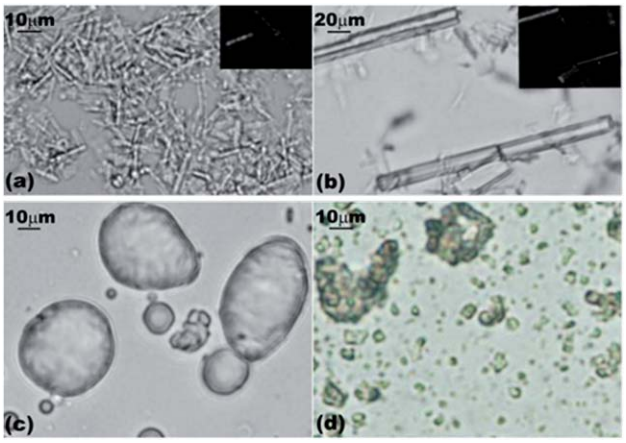

Fig. 12 Optical microscopy images of α-CD and β-CD hexadecane ICs captured at different times: (a) α-CD-hexadecane IC precipitates immediately after dispersion; (b) α-CD-hexadecane IC microrods after 3 days; (c) β-CD-hexadecane IC structures immediately after dispersion; and (d) β-CD-hexadecane IC microcrystals after 3 days.

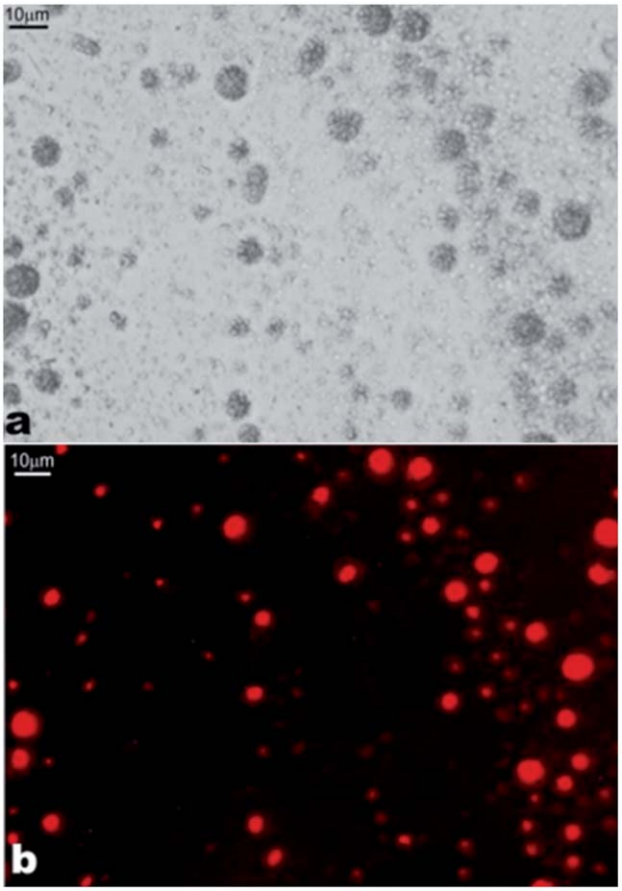

Fig. 13 Images of the β-CD–tetradecane IC structures doped with Nile Red. (a) Optical micrograph; and (b) fluorescence microscopy image with the TRITC filter set. Nile Red fluorescence was observed using the TRITC filter set. Scale bars are 10 μm.

Emulsion stabilisation by formation of CD–tetradecane inclusion complexes. We did some water-in-oil emulsions with silicone oil, sunflower oil, squalane, and isopropyl myristate in the presence of α-CD, β-CD and γ-CD in the aqueous phase as well as oil-in-water emulsions with hexane, tetradecane and hexadecane with α-CD or β-CD in the aqueous phase. In all of these cases, except hexane, we obtained Pickering emulsions at high CD concentrations. We will present these results in a follow up publication. In the case when the CDs do not form stable inclusion complexes with the oil, emulsions are not stable and we cannot claim that this stabilisation mechanism is relevant for any oil. Nevertheless, for a range of different oils, the stabilisation of emulsions based on formation of particles of inclusion complexes with soluble CDs gives enough scope for developing green formulations without the use of surfactants.

Conclusions

We have demonstrated that the shape and size of aggregates from pseudo poly(rotaxane) of *n*-tetradecane can be tuned by the type of CD threaded along its chain length. We discovered that the α-CD inclusion complex (IC) with *n*-tetradecane preferentially forms long thin microrods which self-assemble further into lamella sheets in aqueous solutions. In contrast, the interaction of β-CD and *n*-tetradecane yielded short structures of various cross-sectional areas and these heaped up to preferentially give spherical structures in aqueous solutions. We observed "Janus microrods" when α-CD–tetradecane IC structures were examined under cross-polarised light microscopy, indicating separated crystalline and amorphous regions with varying birefringence. On the other hand, β-CD–tetradecane IC structures did not show any birefringence at all which indicates the presence of amorphous structures. Therefore, the IC crystallinity can also be tuned by selection of CD size.

We also studied the effect of temperature, pH, chaotropic agent concentration and the length of the guest molecule on the formation of microcrystals of ICs with cyclodextrins. The results are important for understanding of the process of encapsulation of non-polar guest molecules in cyclodextrins which have applications in a range of cosmetics and pharmaceutical formulations. The formation of anisotropic microrods from cyclodextrin–oil ICs can also have important implications for the way of stabilisation of some oil-in-water emulsions in the presence of cyclodextrins.

Acknowledgements

B.G.M. thanks Botswana College of Agriculture for financial support of this work as a part of his PhD studies. We thank Mr Tony Sinclair for the preparation and imaging of the SEM samples and Ann Lowry for producing the TEM images.

Notes and references

1 K. Miyake, S. Yasuda, A. Harada, J. Sumaoka, M. Komiyama and H. Shigekawa, *J. Am. Chem. Soc.*, 2003, **125**, 5080–5085.
2 Y. He, X. Shen, Q. Chen and H. Gao, *Phys. Chem. Chem. Phys.*, 2011, **13**, 447–452.
3 B. Jing, X. Chen, X. Wang, C. Yang, Y. Xie and H. Qiu, *Chem.–Eur. J.*, 2007, **13**, 9137–9142.
4 J. Szejtli, *Chem. Rev.*, 1998, **98**, 1743–1754.
5 F. Trotta, M. Zanetti and R. Cavalli, *Beilstein J. Org. Chem.*, 2012, **8**, 2091–2099.
6 M. V. Rekharsky and Y. Inoue, *Chem. Rev.*, 1998, **98**, 1875–1918.
7 M. Bonini, S. Rossi, G. Karlsson, M. Almgren, P. Lo Nostro and P. Baglioni, *Langmuir*, 2006, **22**, 1478–1484.
8 S. Muthusubramanian, A. K. Tiwari, Sonu and S. K. Saha, *Soft Matter*, 2012, **8**, 11072–11084.
9 T. Uyar, C. C. Rusa, M. A. Hunt, E. Aslan, J. Hacaloglu and A. E. Tonelli, *Polymer*, 2005, **46**, 4762–4775.
10 T. V. Frank van de Manakker, C. F. van Nostrum and W. E. Hennink, *Biomacromolecules*, 2009, **10**, 3157–3175.
11 R. Krishnan and K. R. Gopidas, *J. Phys. Chem. Lett.*, 2011, **2**, 2094–2098.
12 W.-C. Chen, S.-W. Kuo, C.-H. Lu, U. S. Jeng and F.-C. Chang, *Macromolecules*, 2009, **42**, 3580–3590.
13 C. P. A. Anconi, C. S. Nascimento, W. B. De Almeida and H. F. Dos Santos, *J. Phys. Chem. C*, 2012, **116**, 18958–18964.
14 G. Wenz, B.-H. Han and A. Müller, *Chem. Rev.*, 2006, **106**, 782–817.
15 A. Harada, J. Li, T. Nakamitsu and M. Kamachi, *J. Org. Chem.*, 1993, **58**, 7524–7528.
16 C. Lv, X. Chen, B. Jing, Y. Zhao and F. Ma, *J. Colloid Interface Sci.*, 2010, **351**, 63–68.
17 A. E. Tonelli, *Beilstein J. Org. Chem.*, 2012, **8**, 1318–1332.
18 L. Jingye, Y. Deyue and C. Qun, *Sci. China, Ser. B: Chem.*, 2002, **45**, 73–83.
19 C.-W. Tu, S.-W. Kuo and F.-C. Chang, *Polymer*, 2009, **50**, 2958–2966.
20 C. Cheng, X.-J. Han, Z.-Q. Dong, Y. Liu, B.-J. Li and S. Zhang, *Macromol. Rapid Commun.*, 2011, **32**, 1965–1971.
21 R. Guo and L. D. Wilson, *Curr. Org. Chem.*, 2013, **17**, 14–21.
22 E. Libowitzky, in *Spectroscopic Methods in Mineralogy IEMU Notes in Mineralogy*, ed. A. Baren, Eötvös University, Budapest, 2004, vol. 6, pp. 227–279.
23 G. Fang, H. Li, F. Yang, X. Liu and S. Wu, *Chem. Eng. J.*, 2009, **153**, 217–221.

